Available online at www.sciencedirect.com
ScienceDirect
Journal of Non-Crystalline Solids 354 (2008) 25–31
JOURNAL OF NON-CRYSTALLINE SOLIDS
www.elsevier.com/locate/jnoncrysol

Generation and annealing of defects in virgin fused silica (type III) upon ArF laser irradiation: Transmission measurements and kinetic model

Ch. Mühlig *, H. Stafast, W. Triebel

Institute of Photonic Technology, Albert-Einstein-Strasse 9, D-07749 Jena, Germany

Received 7 August 2006; received in revised form 18 July 2007
Available online 19 September 2007

Abstract

The transmission of ArF laser pulses in virgin fused silica (type III) samples changes during $N = 10^6$ pulses at an incoming fluence $H_{in} = 5\ mJ\ cm^{-2}\ pulse^{-1}$. The related absorption is determined by the pulse energy absorption coefficient $\alpha(N, H_{in})$ using a modified Beer's law, yielding initial values α_{ini} around $0.005\ cm^{-1}$, a maximum $\alpha_{max} \leqslant 0.02\ cm^{-1}$ at $N = 10^3$–10^4 and stationary values $0.0045\ cm^{-1} \leqslant \alpha_{end} \leqslant 0.0094\ cm^{-1}$ after $N \approx 6 \times 10^5$ pulses. The development $\alpha(N, H_{in} = const.)$ is simulated by a rate equation model assuming a pulse number dependent E' center density $E'(N)$. $E'(N)$ is determined by a dynamic equilibrium between E' center generation and annealing. Generation occurs photolytically from the precursors ODC II and unstable SiH structures upon single photon absorption and from strained SiO bonds via two-photon excitation. Annealing in the dark periods between the laser pulses is dominated by the reaction of E' with H_2 present in the SiO_2 network. The development $\alpha(N, H_{in} = const.)$ is observed for the very first sample irradiation only (virgin state). The values α_{end} are not accessible by simple spectrophotometer measurements.

PACS: 42.70.Ce; 61.80.Ba; 81.05.Kf; 78.20.Bh

Keywords: Hydrogen in glass; Measurement techniques; Optical spectroscopy; Modeling and simulation; Optical properties; Absorption; Optical spectroscopy; Photoinduced effects; Silica; Defects

1. Introduction

Synthetic fused silica is currently the most widely used lens material in deep ultra-violet (DUV) applications, such as DUV optical lithography and excimer laser microfabrication. In optical lithography the printing of ever smaller features required to reduce the wavelength from 436 nm (g-line) and 365 nm (i-line) obtained from high pressure continuous Hg discharge lamps to 248 nm (KrF laser), and more recently, to 193 nm (ArF laser) obtained from pulsed lasers [1,2]. Well collimated beams of narrow bandwidth are applied at low fluences in the 0.1–10 mJ cm^{-2} $pulse^{-1}$ range. In laser microfabrication, on the other hand, high fluences above the ablation threshold of typically >1 J cm^{-2} $pulse^{-1}$ are necessary and typically achieved in focussed beams without spectral narrowing.

Generally, DUV laser pulses imply peak intensities which are high enough to induce two photon absorption and optical degradation in fused silica. Over long irradiation periods this yields an absorption increase due to defect formation and a refractive index change due to microscopic structural rearrangements limiting the lifetime of optical components. In order to proof and to model the long term laser stability of fused silica, material tests are carried out with up to 10^{10} laser pulses and intermediate transmission and/or refractive index measurements [3–8]. Besides long term optical degradation, however, it is necessary to investigate the optical properties on the much shorter

* Corresponding author.
E-mail address: christian.muehlig@ipht-jena.de (Ch. Mühlig).

0022-3093/$ - see front matter © 2007 Elsevier B.V. All rights reserved.
doi:10.1016/j.jnoncrysol.2007.07.019

second-to-minute time scale, commonly depicted as rapid damage regime [9,10]. In particular, relatively rapid absorption changes, induced e.g. by switching the fluence or repetition rate, may affect the illumination dose on the photo resist in lithographic fabrication. Furthermore, absorption changes will vary the temperature distribution in the optical system and diminish the spatial imaging resolution. Finally it is pointed out that rapid damage has to be considered carefully when laying down the specification test procedures: ArF laser irradiation of fused silica in its virgin state, i.e. the very first irradiation, induces considerable absorption changes on the minute time scale [9,10].

In this work, ArF laser transmission measurements are applied to quantitatively investigate the absorption changes in virgin fused silica (type III) upon the first 10^6 laser pulses. The measured absorption behavior is simulated by kinetic modelling the E' center generation and annealing.

2. Experimental

The investigated fused silica samples from Schott Lithotec AG, Jena, are of type III (OH content >1000 ppm) prepared by flame hydrolysis of high purity synthetic raw material. Sample 1 is defined as excimer grade material whereas samples 2 and 3 are of experimental grade. In sample 3 the hydrogen content is reduced compared to samples 1 and 2. All samples have a cross section of $25 \times 25\ \mathrm{mm}^2$ and a length of 300 mm and their relevant polished surfaces are cleaned with pure ethanol prior to laser irradiation.

The experiments are carried out at room temperature in a nitrogen purged experimental setup using an ArF laser (LPX 240i, Lambda Physik). The laser beam is shaped by an aperture in front of the sample to a cross section of $15 \times 5\ \mathrm{mm}^2$ with a top-hat like intensity profile. The samples are irradiated at the incoming fluence $H_{\mathrm{in}} = 5\ \mathrm{mJ\ cm^{-2}\ pulse^{-1}}$ that is small enough to keep two-photon absorption at a low level and to achieve a stationary absorption behavior within an experimentally reasonable number of laser pulses $N = 6.5 \times 10^6$. The repetition rates of 150 Hz for the *in situ* transmission measurements and 200 Hz for irradiation represent the upper experimental limits for the transmission measurements (limit of detector heads) and for minimum variations of the irradiation conditions from pulse to pulse, respectively. At the irradiation end, equal to a total irradiation dose of $3.25\ \mathrm{kJ\ cm^{-2}}$, the gradient $\mathrm{d}\alpha/\mathrm{d}N < 10^{-8}\ \mathrm{cm^{-1}\ pulse^{-1}}$ is regarded small enough to estimate the α_{end} value.

For *in situ* transmission measurements the energy of each single laser pulse is recorded simultaneously in front of the sample using a beam splitter (E_{in}) and directly behind the sample (E_{out}) by fast pyroelectric detectors (PE-25 H, OPHIR Optronics, Inc.) which are calibrated by the supplier for 193 nm relative to a NIST traceable standard. The ratios $E_{\mathrm{out}}/E_{\mathrm{in}}$ of 50 consecutive laser pulses are averaged. The obtained absolute transmission accuracy ΔT is better than $\pm 0.2\%$ which transforms into the accuracy $|\Delta\alpha| \leqslant 0.0001\ \mathrm{cm^{-1}}$ for the absorption coefficient.

3. Results

The measured laser pulse energy values E_{in} and E_{out} are easily converted to fluence values H_{in} and H_{out}, respectively. The fluence H is considered as a measure of the average laser pulse intensity I particularly if the temporal laser beam profile stays constant. Consequently it is very common and convenient to convert Beer's law to $\mathrm{d}H(z)/\mathrm{d}z = -\alpha H(z)$ in order to describe the fluence attenuation along the sample length axis z. Keeping in mind that light scattering and nonlinear absorption are very small in the highly transparent samples it appears appropriate to consider α as the absorption coefficient which is constant throughout the sample length. Taking furthermore into account that the optical sample properties vary during (prolonged) irradiation by a laser pulse series and that absorption is affected by two-photon absorption, the absorption coefficient is described as a function of the laser pulse number N and incoming fluence H_{in}, i.e. $\alpha = \alpha(N, H_{\mathrm{in}})$. This leads to the modified Beer's law

$$\mathrm{d}H(z)/\mathrm{d}z = -\alpha(N, H_{\mathrm{in}})H(z). \tag{1}$$

Integration of Eq. (1) yields $\alpha(N, H_{\mathrm{in}}) = -1/z \ln(H_{\mathrm{out}}/H_{\mathrm{in}})$. The ratio $H_{\mathrm{out}}/H_{\mathrm{in}}$ can be replaced by $T(N, H_{\mathrm{in}})/T_{\max}$ with $T(N, H_{\mathrm{in}})$ being the sample transmission determined from the laser pulse energies E_{in} and E_{out} of the laser pulse number N irradiating with fluence H_{in}. $T_{\max}$ is the ideal laser pulse transmission without any absorption and scattering by the sample but Fresnel reflection at the beam entrance and exit surfaces. Thus we achieve the following relation between $\alpha(N, H_{\mathrm{in}})$ and the experimental value $T(N, H_{\mathrm{in}})$:

$$\alpha(N, H_{\mathrm{in}}) = -1/z \ln(T(N, H_{\mathrm{in}})/T_{\max}). \tag{2}$$

The development of the laser energy absorption coefficient $\alpha(N, H_{\mathrm{in}})$ with the pulse number N upon ArF laser irradiation is qualitatively the same for all investigated virgin fused silica samples (Figs. 1 and 2). The first measurement value $\alpha(1\text{–}50, H_{\mathrm{in}})$ is defined as initial absorption coefficient α_{ini}, which is assumed to be close to the value of the virgin sample, e.g. measured by a spectrophotometer. The results yield $\alpha_{\mathrm{ini}}\ (\text{sample } 3) = 0.0041 < \alpha_{\mathrm{ini}}\ (\text{sample } 1) = 0.0058\ \mathrm{cm^{-1}} < \alpha_{\mathrm{ini}}\ (\text{sample } 2) = 0.0065\ \mathrm{cm^{-1}}$. Within the first 10^3–10^4 laser pulses $\alpha(N, H_{\mathrm{in}})$ rises to a maximum value $\alpha_{\max}$ (Fig. 1). The difference $\alpha_{\max} - \alpha_{\mathrm{ini}} = 0.0040\ \mathrm{cm^{-1}}$ of sample 1 is considerably smaller than the related values of $0.0074\ \mathrm{cm^{-1}}$ and $0.0164\ \mathrm{cm^{-1}}$ for samples 2 and 3, respectively. The same ranking is found if the absolute $\mathrm{d}\alpha/\mathrm{d}N$ slope values are considered. During further irradiation the absorption decreases towards a stationary value (Fig. 2) and the last measurement value is defined as α_{end}. In contrast to the irradiation start sample 2 now exhibits the lowest value $\alpha_{\mathrm{end}} = 0.0045\ \mathrm{cm^{-1}}$ compared to $\alpha_{\mathrm{end}} = 0.0057\ \mathrm{cm^{-1}}$ and $\alpha_{\mathrm{end}} = 0.0094\ \mathrm{cm^{-1}}$ for samples 1 and 3,

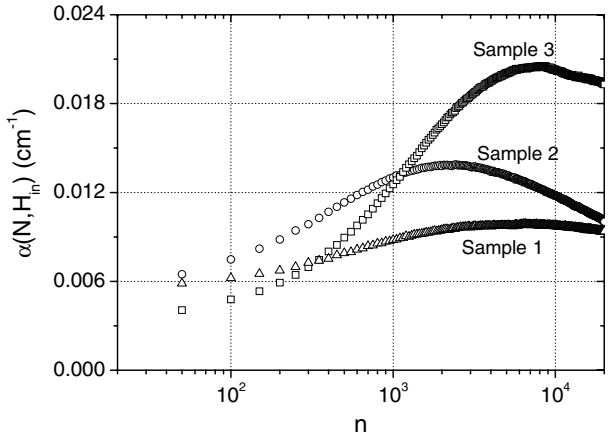

Fig. 1. ArF laser energy absorption coefficients $\alpha(N, H_{in})$ of virgin fused silica samples determined at a fluence of 5 mJ cm^{-2} pulse^{-1} and 150 Hz repetition rate as a function of the laser pulse number $N \leqslant 2 \times 10^4$. The accuracy of the absorption data is $|\Delta\alpha| \leqslant 0.0001$ cm^{-1}.

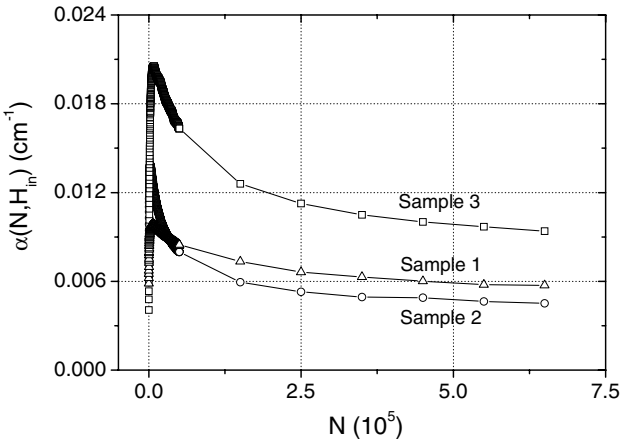

Fig. 2. ArF laser energy absorption coefficients $\alpha(N, H_{in})$ of virgin fused silica samples determined at a fluence of 5 mJ cm^{-2} pulse^{-1} and 150 Hz repetition rate as a function of the laser pulse number $N \leqslant 6.5 \times 10^5$; the straight lines for $N > 2 \times 10^4$ represent irradiation at 200 Hz repetition rate between the measurement points. The accuracy of the absorption data is $|\Delta\alpha| \leqslant 0.0001$ cm^{-1}.

respectively. It is pointed out that the values of samples 2 and 3 are the highest and lowest at the beginning and turn to the lowest and highest values at the end, respectively. It is remarkable that the absorption α_{end} of sample 2 at the irradiation end is smaller than the initial value α_{ini}. A summary of the α_{ini}, α_{max} and α_{end} values is given in Table 1.

Table 1
ArF laser energy absorption coefficients $\alpha(N, H_{in})$ (cm^{-1}) of fused silica samples during irradiation with $N = 6.5 \times 10^5$ laser pulses at a fluence of 5 mJ cm^{-2} pulse^{-1} (data from Figs. 1 and 2) determined at the beginning (α_{ini}), the intermediate maximum (α_{max}) and the end (α_{end}) with error limits $|\Delta\alpha| \leqslant 0.00015$ cm^{-1}

Sample	α_{ini}	α_{max}	α_{end}
1	0.0058	0.0098	0.0057
2	0.0065	0.0139	0.0045
3	0.0041	0.0205	0.0094

The observed absorption development is irreversible: when repeating the experiment after a couple of days, $\alpha(N, H_{in})$ very quickly reaches its final value α_{end} obtained in the very first laser irradiation sequence and then remains constant.

4. Model

Single photon absorption in the UV/DUV spectral region by synthetic fused silica of high purity is mainly attributed to three intrinsic defects known from literature [11], the oxygen deficient centers (ODC), the non-bridging oxygen hole centers (NBOH), and the E' centers. Looking at their absorption cross sections at the ArF laser wavelength of 193 nm (Fig. 3) the E' center dominates by far and therefore has been implemented in the following absorption development model.

To simulate the $\alpha(N, H_{in})$ development with the number of laser pulses N as displayed in Figs. 1 and 2 our model focuses on the generation of E' centers during the ArF laser pulses and their annealing during the intermediate dark periods between the laser pulses. For convenience Fig. 4 shows the temporal scheme underlying the simulation model. $[E']_0$ is the initial density of E' states prior to the first laser pulse, which is assumed to be negligible for the selected fused silica samples, i.e. $[E']_0 = 0$. ArF laser absorption during the first pulse of duration τ_L is described by $\alpha(N = 1, H_{in} = 5$ mJ/cm^2 pulse$^{-1})$, abbreviated by α_1, leading to an increase $\Delta_1[E']_g$ of $[E']$ due to defect generation (index g). In the subsequent dark period of duration τ_a the $[E']$ value decreases about $\Delta_1[E']_a$ due to annealing (index a). The total change of $[E']$ between the start of the first and the start of the second laser pulse amounts to $\Delta_1[E'] = \Delta_1[E']_g - \Delta_1[E']_a$, i.e. $[E']_1 = [E']_0 + \Delta_1[E']$, or more generally

$$[E']_N = [E']_{N-1} + \Delta_N[E'], \tag{3}$$

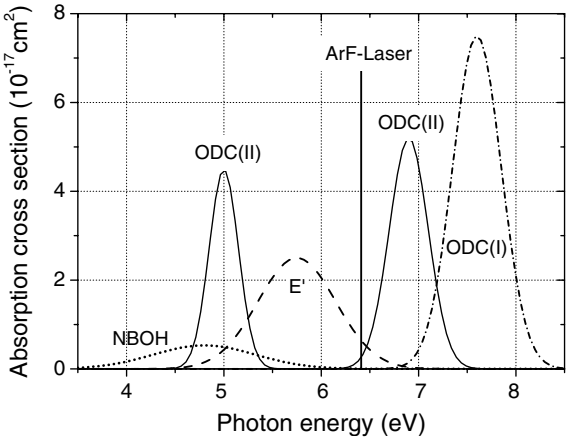

Fig. 3. Optical absorption bands of the NBOH (non-bridging oxygen hole), ODC (oxygen deficient center) and E' defect centers in fused silica [12].

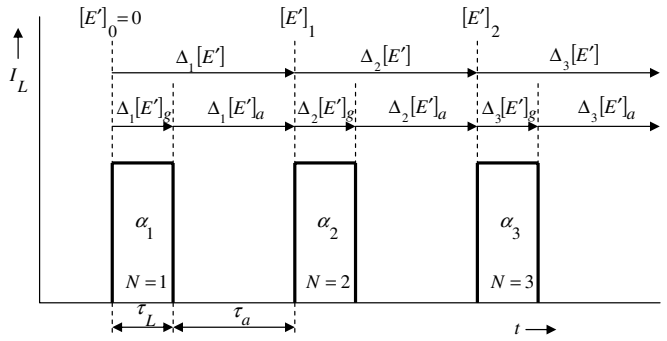

Fig. 4. Temporal scheme of E' center generation during ArF laser pulses of duration τ_L and E' center annealing within the time τ_a between consecutive laser pulses (cf. text).

with

$$\Delta_N[E'] = \Delta_N[E']_g - \Delta_N[E']_a. \quad (4)$$

The change of $[E']$ from pulse to pulse is reflected by a change of the absorption coefficient, i.e. individual α_N values apply to the individual laser pulses of number N. The calculation of the α_N development with N is based on the calculations of the $\Delta_N[E']$ values and their relation to α_N which are described in the following.

The E' generation during the laser pulses is induced by photolytic conversion of oxygen deficient centers ODCII (precursors P_1 and P_2) [11–13], of unstable SiH structures (precursor P_3) [9] and of strained bonds in the SiO_2 matrix (precursor P_4) [14–16]. The conversion of precursors P_1 to P_3 occurs via single photon absorption whereas the conversion of P_4 requires a two photon absorption process. The E' center generation term then has the structure

$$\Delta_N[E']_g = \sum_i [P_i]_{N-1} \cdot \exp(-k_i \cdot \tau_L), \quad (5)$$

where $[P_i]_{N-1}$ denotes the concentration of convertable precursor P_i before laser pulse N and $k_i = k_i(H_{in})$ the related conversion rate constant. The rate constants $k_1(H_{in} = 5\ \text{mJ cm}^{-2}\ \text{pulse}^{-1}) = 2 \times 10^3\ \text{s}^{-1}$ and $k_2(H_{in} = 5\ \text{mJ cm}^{-2}\ \text{pulse}^{-1}) = 2 \times 10^4\ \text{s}^{-1}$ can be derived from fluorescence measurements (cf. discussion). The initial precursor densities $[P_1]_0$, $[P_2]_0$, and $[P_3]_0$ as well as k_3 are obtained from the curve fitting procedure (cf. below). Precursor P_4 is known to be responsible for the absorption increase in fused silica over long irradiation periods by laser induced transformation into E' and NBOH centers [7]. At low fluences $H < 5\ \text{mJ cm}^{-2}\ \text{pulse}^{-1}$ this absorption increase typically lasts more the 10^9 laser pulses until all precursors P_4 in the irradiated sample volume have been transformed [3]. Thus, taking into account the applied pulse number $N < 10^6$ in the presented experiments, the original density $[P_4]_0$ is considered constant throughout the applied pulse series. This yields a constant E' generation $\eta\ [P_4]_0$ ($\eta \ll 1$) per pulse from strained bonds, which is obtained from the curve fitting procedure.

E' annealing between the laser pulses due to the reaction with molecular hydrogen is expressed by

$$\Delta_N[E']_a = \left([E']_{N-1} + \Delta_N[E']_g\right) \cdot \exp(-k_a \cdot \tau_a), \quad (6)$$

with the annealing rate constant k_a, which is obtained from the curve fitting procedure.

The absorption coefficient α_N relevant for laser pulse N is connected to the density $[E']_{N-1}$ by the relation $\alpha_N = \sigma(E', 193\ \text{nm}) \cdot [E']_{N-1}$ with $\sigma(E', 193\ \text{nm}) = 8 \times 10^{-18}\ \text{cm}^2$ (mean value from literature data [11,12]). Looking at the effect of successive laser pulses, the following recurring formula can be derived:

$$\alpha_N = \sigma(E') \cdot A^{N-1} \left[\sum_{i=1}^{2} \left(B_i \cdot \sum_{j=0}^{N-1} C_i^j A^{-j} \right) + D \cdot \sum_{j=0}^{N=1} A^{-j} + B_3 \cdot \sum_{j=0}^{N=1} C_3^j A^{-j} \right]. \quad (7)$$

Inserting the solutions for finite geometric series into Eq. (7) yields the final expression for α_N:

$$\alpha_N = \sigma(E') \cdot \left(\sum_{i=1}^{2} \frac{B_i}{C_i - A} (C_i^N - A^N) + \frac{D}{1-A}(1 - A^N) + \frac{B_3}{C_3 - A}(C_3^N - A^N) \right), \quad (8)$$

with the abbreviations $A = \exp(-k_a \cdot \tau_a)$, $B_i = [P_i]_0(1 - \exp(-k_i \cdot \tau_L))$, $C_i = \exp(-k_i \cdot \tau_L)$ and $D = \eta[P_4]_0$ ($\eta \ll 1$). For all investigated samples the experimental data can be adapted very well by using Eq. (8). For example, applying Eq. (8) to the α_N curve of sample 3 (Fig. 2) setting $\alpha_0 = 0$, varying the parameters $[P_1]_0$, $[P_2]_0$, $[P_3]_0$, $\eta\ [P_4]_0$, k_3, and k_a by following the least squares method yields the fitting curve displayed in Fig. 5 together with the values for the above parameters as summarized in Table 2. The same procedure applied to the α_N curves of samples 1 and 2 yields fitting curves of comparable quality and the parameter values given in Table 2.

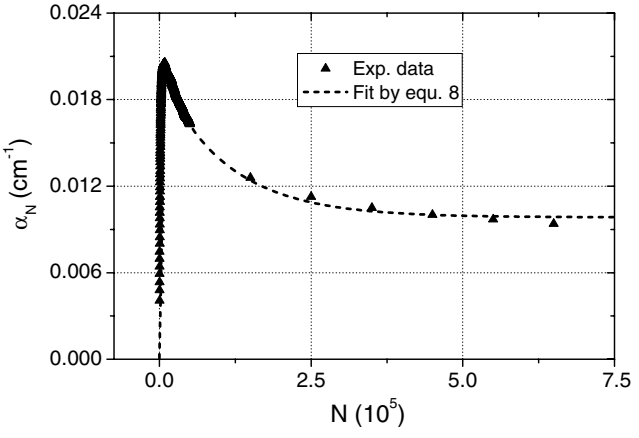

Fig. 5. Fit of the experimental data α_N of sample 3 in Fig. 2 by Eq.(8).

Table 2
Material parameters for samples 1–3 obtained from fits of the experimental results (Figs. 1 and 2) using Eq. (8) The relative error for the parameters is estimated to $\leqslant 10\%$

Sample	$[P_1]_0$ (cm^{-3})	$[P_2]_0$ (cm^{-3})	$[P_3]_0$ (cm^{-3})	$\eta \cdot [P_4]_0$ (cm^{-3} $pulse^{-1}$)	k_a (s^{-1})	k_3 (s^{-1})
1	3.3×10^{14}	5.2×10^{16}	2.5×10^{17}	2.3×10^{12}	0.66	240
2	3.2×10^{13}	2×10^{15}	3×10^{17}	3.2×10^{12}	0.78	241
3	1.2×10^{13}	3×10^{15}	1.1×10^{17}	1.1×10^{12}	0.14	300

5. Discussion

The following discussion is dealing with the comparison between the model calculation and the experimental data (5.1), the comparison of the calculated material parameters with literature values (5.2) and the sensitivity of the model results to material parameter variations (5.3).

5.1. Comparison between model calculation and experimental data

The measured change of the ArF laser absorption by the selected fused silica samples during the first 10^6 laser pulses is assumed to be dominated by the E' center absorption development. In the above model the density $[E']$ is determined by the dynamic equilibrium between E' center formation during the ArF laser pulses and their annealing in the dark periods. The generation of E' centers is based on different precursors (P_1 to P_4) obtained during manufacturing. The annealing is due to the reaction of E' centers with interstitial molecular hydrogen.

At the beginning of ArF laser irradiation all samples show an instantaneous absorption $\alpha_{ini} > 0$ in agreement with spectrometer measurements. The data from Tables 1 and 2 reveal a good correlation between these α_{ini} values and the sum $([P_1]_0 + [P_2]_0 + [P_3]_0)$ related to the initial ODCII and unstable SiH densities, respectively. In particular, it appears from Table 2 that unstable SiH bonds play the major role for the ArF laser absorption in the selected virgin samples. This underlines that single photon absorption is dominant in virgin fused silica for the applied laser pulse fluence $H = 5\ mJ\ cm^{-2}\ pulse^{-1}$. The sum $([P_1]_0 + [P_2]_0 + [P_3]_0)$ is very similar for samples 1 and 2 ($\sim 3 \times 10^{17}\ cm^{-3}$) resulting in comparable α_{ini} values of $5.8 \times 10^{-3}\ cm^{-1}$ and $6.5 \times 10^{-3}\ cm^{-1}$, whereas sample 3 shows lower values of $1.1 \times 10^{17}\ cm^{-3}$ and $4.1 \times 10^{-3}\ cm^{-1}$, respectively. These results support the model assumption $[E']_0 = 0$ but demand a model extension by adding a precursor related initial absorption that diminishes strongly upon the first ArF laser irradiation due to the precursor transformation into E' centers.

During the first 10^4 pulses of ArF laser irradiation the precursor conversion results in a fast accumulation of E' centers, i.e. in a rapid absorption increase. The latter, however, lowers with the number of pulses due to the decreasing precursor densities $[P_1]$ to $[P_3]$. As a result, the absorption reaches an intermediate α_{max} value which depends on both the precursor densities and the annealing rate. Sample 3 shows the highest α_{max} value ($0.0205\ cm^{-1}$, followed by sample 2 ($0.0139\ cm^{-1}$) and sample 1 ($0.0098\ cm^{-1}$). From Table 2 it is seen that the annealing rate constant k_a of sample 3 is about a factor of 5 smaller than the k_a values of samples 1 and 2. It is assumed that this results in the much higher α_{max} value of sample 3 compared to samples 1 and 2. In contrast, the lower intermediate α_{max} value of sample 1 compared to sample 2 is probably due to the lower $[P_3]_0$ and $\eta\ [P_4]_0$ values of sample 1.

For all investigated samples laser irradiation beyond the intermediate α_{max} values results in an absorption decrease which lowers with increasing pulse number. At the irradiation end ($N = 6.5 \times 10^5$ pulses) the absorption appears to reach a stationary level denoted as α_{end}. It is seen from Table 1 that the α_{end} values do not correlate with the α_{ini} data, i.e. with the sum $([P_1]_0 + [P_2]_0 + [P_3]_0)$ related to the initial ODCII and unstable SiH densities. That means that absorption data of virgin fused silica, typically measured by spectrometers, are not necessarily 'reliable' figures of merit with respect to the evaluation of fused silica for ArF laser applications. Comparing the material parameters in Table 2 however, the annealing rates k_a are assumed to be the major reason for the different α_{end} data. The calculated k_a value of sample 3 is about a factor of 5 smaller than those of samples 1 and 2. This is in agreement with the reduced molecular hydrogen content in sample 3. As a result sample 3, even though having the lowest constant E' generation rate per pulse $\eta\ [P_4]_0$ of all samples, shows an α_{end} value ($0.0094\ cm^{-1}$) that is significantly larger than α_{end} for samples 1 ($0.0057\ cm^{-1}$) and 2 ($0.0045\ cm^{-1}$), respectively.

5.2. Comparison of calculated material parameters with literature values

The fixed parameter: $\sigma(E', 193\ nm) = 8 \times 10^{-18}\ cm^2$ has been derived as a mean value from several literature data [11,12]. The parameters $k_1 = 2 \times 10^3\ s^{-1}$ and $k_2 = 2 \times 10^4\ s^{-1}$ were calculated from the measured decay of the two ODCII fluorescence bands upon ArF laser irradiation [17]. Furthermore, the initial E' density as obtained from manufacturing was neglected, that is $\alpha_0 = 0$. The remaining material parameters (Table 2) were obtained from the fitting procedures and deserve a critical review in comparison to literature values.

The individual sums $([P_1]_0 + [P_2]_0)$ are related to the individual initial ODCII densities and found to lie in the

10^{15}–10^{16} cm^{-3} range. These values are in agreement with the theoretically estimated concentrations of up to some 10^{16} cm^{-3} ODCII defects in stoichiometric fused silica loaded with hydrogen [18]. The calculated values for the E' center increase per pulse from strained SiO bonds, η $[P_4]_0$, are about 2–3 orders of magnitude higher than the literature data for hydroxyl-free fused silica ([OH] < 1 ppm) [19]. Increasing the OH content, however, raises the η $[P_4]_0$ values. A value η $[P_4]_0 \sim 2 \times 10^{12}$ cm^{-3} $pulse^{-1}$ was found for ArF laser irradiation of fused silica with [OH] = 20 ppm at a fluence of 35 mJ cm^{-2} $pulse^{-1}$ [18]. This corresponds to η $[P_4]_0 \sim 4 \times 10^{10}$ cm^{-3} $pulse^{-1}$ for $H = 5$ mJ cm^{-2} $pulse^{-1}$ in the present study if taking into account a quadratic fluence dependence of the two photon absorption process for the E' center generation from strained SiO bonds. A linear extrapolation to [OH] ~1000 ppm of the samples in this study yields η $[P_4]_0$ $\sim 2 \times 10^{12}$ cm^{-3} $pulse^{-1}$ in agreement with the values in Table 2.

Looking at E' annealing, two rate values are discussed in the literature. For the annealing of newly generated E' centers by molecular hydrogen the rates range from 0.01 to 0.1 s^{-1} [9]. E' centers generated from SiH bonds, however, are annealed by atomic hydrogen (gemini pair $E' + H$) at higher rates in the 10 s^{-1} range [9]. The k_a values between 0.1 and 0.8 s^{-1} in the present study are slightly above those found for E' center annealing by molecular hydrogen. This reveals that E' center annealing during the first ArF laser irradiation period with approximately 10^6 pulses is probably dominated by molecular hydrogen. Finally, no data for the parameters $[P_3]_0$ and k_3 related to the unstable SiH modification, are so far available in the literature.

5.3. Sensitivity of model results to material parameter variation

To study the influence of the selected material parameters on the modelled absorption values α_N following Eq. (8) the parameters $[P_1]_0$, $[P_2]_0$ $[P_3]_0$, η $[P_4]_0$ and k_a obtained from the fitting curves are varied individually by 20%. Raising the $[P_1]_0$ or the $[P_2]_0$ value by 20% has no apparent effect. Only when reaching the order of magnitude of the $[P_3]_0$ density, i.e. an increase by at least a factor of 10, the ODCII density yields a relevant change in the absorption course. Changing the parameters $[P_3]_0$, η $[P_4]_0$ or k_a yields significant effects as exemplified for sample 3 in Fig. 6(a) and (b).

Figs. 6(a) and (b) show that an increased initial density $[P_3]_0$ of unstable SiH bonds raises the absorption coefficient only within the first time interval. At higher pulse numbers N with $N \cdot \eta \cdot [P_4]_0 > [P_3]_0$ the absorption behavior and thus the final absorption coefficient α_{end} remains unchanged. This is in good agreement with the results in Section 5.1 showing that the original density $[P_3]_0$ does not affect the α_{end} values. Raising the η $[P_4]_0$ value by 20%, however, results in a permanent absorption coefficient increase. Particularly in the final part, when the E' generation from

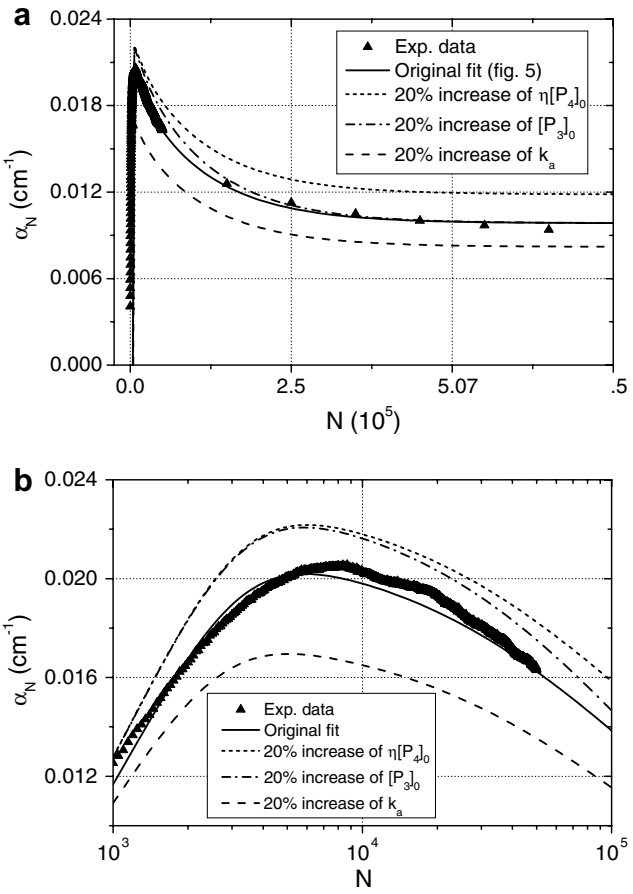

Fig. 6. Changes of the α_N fitting curve of Fig. 5 upon variations of the material parameters $[P_3]_0$, $\eta \cdot [P_4]_0$ and k_a (cf. insets) (a) α_N curve of sample 3 from Fig. 2, (b) α_N curve of sample 3 for $10^3 \leqslant N \leqslant 10^5$ plotted versus a logarithmic abscissa scale.

ODCII and unstable SiH bonds is terminated to a great extent, the influence of strained SiO bonds becomes high and α_{end} follows the η $[P_4]_0$ value. The most significant change of α_N, however, arises from increasing the annealing rate constant k_a. The α_N data decrease throughout the entire irradiation time by the same percentage as the annealing rate increases. Again, the explanation for the measured experimental data in Section 5.1 is confirmed: the annealing has a strong impact on the intermediate α_{max} and the final α_{end} values.

6. Summary and conclusions

The transparency of synthetic fused silica of type III for an ArF laser beam was studied during a series of about 10^6 pulses. The pulse energy absorption was quantified via a modified Beer's law. In this modification the light intensity I was replaced by the pulse energy fluence H. The related absorption coefficient $\alpha(N, H_{in})$ was considered to be a function of the laser pulse number N and the incoming fluence H_{in}. The $\alpha(N, H_{in})$ values recorded at $H_{in} = 5$ mJ cm^{-2} $pulse^{-1}$ ranged from 4×10^{-3} to 2×10^{-2} cm^{-1}. Starting from a low level α_{ini}, they exhibited a maximum α_{max} after

about 10^3–10^4 pulses and approached a relatively low stationary value α_{end} after about 6.5×10^5 pulses.

The development of $\alpha(N, H_{in} = 5\ \text{mJ cm}^{-2}\ \text{pulse}^{-1})$ with N was well fitted by a simple rate equation model. In this model it is assumed that these α values are proportional to the E' defect center density. The density $[E']$ is modelled by assuming a dynamic equilibrium between defect generation during the laser pulses and annealing in the dark periods between the laser pulses. Defect generation occurs photolytically from ODC II centers and unstable SiH structures upon single photon absorption and from strained SiO bonds upon two-photon absorption. Annealing is under these conditions dominated by the reaction of the E' defect centers with molecular hydrogen present in the SiO_2 network.

The obtained results are of high practical importance with respect to the evaluation of fused silica for ArF laser applications, particularly for long term applications under constant laser absorption conditions. It has been shown that the initial absorption value α_{ini}, as e.g. measured in spectrophotometers, does not provide a measure of the intermediate and long term performance of the fused silica samples under ArF laser irradiation. Evidently it is necessary to apply a minimum irradiation dose to the material before 'reliable' figures of merit can be extracted from the measurements. For the above fluence $H_{in} = 5\ \text{mJ cm}^{-2}\ \text{pulse}^{-1}$ a minimum pulse number $N_{min} = 6.5 \times 10^5$ appears necessary, i.e. a dose of 3.25 kJ cm^{-2}. It will be very interesting to find out how N_{min} scales with the fluence H in order to design an evaluation procedure particularly in view of the fact that each sample can be used once only.

Finally it is pointed out that the approximations applied to the model for the short and intermediate time developments of the absorption coefficient $\alpha(N, H_{in})$ need not necessarily apply to the 'marathon' test results of fused silica. It is e.g. very likely that the consumption of molecular hydrogen and the formation of SiH bond structures upon prolonged ArF laser irradiation will change the importance of the individual defect generation and annealing processes.

Acknowlegdements

The authors would like to thank the Federal State of Thuringia and the Schott–Jenaer–Glas–Fonds for financial support. The authors are grateful to Schott Lithotec AG Jena for providing the fused silica samples and material's data as well as many hints and fruitful discussions.

References

[1] W. Kaiser, Innovation Special Microelectronics 1, Carl Zeiss Oberkochen (1998).
[2] M. Rothschild, Mater. Today (2005), February.
[3] V. Liberman, M. Rothschild, J.H.C. Sedlacek, R.S. Uttaro, A. Greenville, A.K. Bates, C. Van Peski, Opt. Lett. 24 (1999) 58.
[4] M. Shimbo, T. Nakajima, N. Tsuji, T. Kakuno, T. Obara, Jpn. J. Appl. Phys. 38 (1999) 848.
[5] J.M. Algots, R. Sandstrom, W. Partlo, K. Takahashi, H. Ishii, Y. Hasegawa, Proc. SPIE 5377 (2004) 1815.
[6] V. Liberman, M. Rothschild, J.H.C. Sedlacek, R.S. Uttaro, A. Greenville, J. Non-Cryst. Solids 244 (1999) 159.
[7] U. Natura, O. Sohr, R. Martin, M. Kahlke, G. Fasold, Proc. SPIE 5273 (2003) 155.
[8] U. Natura, O. Sohr, M. Letzt, R. Martin, M. Kahlke, G. Fasold, Proc. SPIE 5377 (2004) 176.
[9] C.M. Smith, N.F. Borrelli, R.J. Araujo, Appl. Opt. 39 (2000) 5778.
[10] U. Natura, R. Martin, G. Gönna, M. Kahlke, G. Fasold, Proc. SPIE 5754 (2005) 1312.
[11] L. Skuja, J. Non-Cryst. Solids 239 (1998) 16.
[12] L. Skuja, H. Hosono, M. Hirano, Proc. SPIE 4347 (2001) 155.
[13] Y. Sakurai, J. Non-Cryst. Solids 271 (2000) 218.
[14] A.R. Silins, L.N. Skuja, A.N. Trukhin, J. Non-Cryst. Solids 38&39 (1980) 195.
[15] Ch. Pfleiderer, N. Leclerc, K.-O. Greulich, J. Non-Cryst. Solids 159 (1993) 145.
[16] W. Triebel, M. Guntau, Ch. Mühlig, A. Wiese, Glass Sci. Technol. 71C (1998) 67.
[17] Ch. Mühlig, S. Kufert, W. Triebel, F. Coriand, Proc. SPIE 4779 (2002) 107.
[18] A. Silins, L. Lace, A. Lukjanska, Latvian J. Phys. Technol. Sci. N5 (1999) 3.
[19] K. Arai, H. Imai, H. Hosono, Y. Abe, H. Imagawa, Appl. Phys. Lett. 53 (1988) 1891.